Analyzing the Turbulent Flow Characteristics by Utilizing k-ϵ Turbulence Model

Md. Safayet Hossain, Md. Ishtiaque Hossain, Somit Pramanik, J.U. Ahamed

***Abstract*—This study attempts to illustrate the behavior of a fully developed turbulent flow by using k-ε turbulence model. A two dimensional smooth bend channel is adopted for this experiment and water was chosen as working fluid. The Reynolds number was gradually increased to predict the diversity in turbulent kinetic energy (TKE), turbulent dissipation rate, turbulent intensity and eddy viscosity. Primarily the flow has been solved by employing three distinct k-ϵ turbulence models namely, Standard, Renormalization-group (RNG) and Realizable model. After experimenting with ten different sample (from 74E03 to 298E03) of Reynolds numbers, each of these analyses explicitly showed that Standard k-ε model gives much higher value of any aforementioned turbulent properties with respect to other two equation turbulence models. Later it's been discovered that TKE obtained from Standard k-ω model is almost same as Realizable k-ε model (for Re=298E03, the difference is about 1.8%). It has been observed that the skin friction coefficient at the bend region obtained from different two equation models (Standard, Realizable and RNG k-ϵ model and Standard k-ω model) are almost similar to each other for each sample of Reynolds number. Quadrilateral elements were taken into consideration for grid generation in this analysis. Also, to decrease cost and to achieve further accuracy as well as reduced time consumption mapped faced meshing was utilized.**

***Index Terms*—CFD; k-ε; k-ω; RNG; Skin Friction Factor; TKE.**

I. INTRODUCTION

In recent times, pipe bends of different angles has become an essential part of any piping network for providing flexibility in many critical routing. Curved pipes are used in several industrial applications such as in heat exchangers, turbine machineries, HVAC appliances etc. Different pipe bend fittings are used in plumbing networks to adapt to different sizes or shapes and this networking system dealt with several engineering problems. Therefore, the investigation of pipe network is very important in engineering point of view. Particularly investigation of the flow through the bend region is very important to understand and improve their performance. Experimentally and numerically various researches had been carried out to study the flow phenomena of bend pipes. Jongtae Kim et al [1] tried to characterize the swirling secondary flow in the downstream of a pipe bend using OpenFOAM CFD package and performed various experimental and numerical simulation based on different turbulence models and found that the RNG k-ε turbulence model gives good results for primary stream wise velocity and secondary swirling velocity profiles compared to other turbulence models. A good predictability for the stream wise velocity components is shown by the non-linear turbulence models but the results provided by those turbulence models in case of secondary swirling velocity components are very weak. Beibei Feng et al investigated pressure distribution in a 90-degree elbow flowing Helium gas through the elbow. By employing k-ω turbulence model they compared the numerical data with the experimental data in this study [2]. Using k-ϵ turbulent model, Prasun Dutta and Nityananda Nand analyzed numerically the turbulent flow of single phase incompressible fluid through 90˚ pipe bend for different Reynolds number. They conveyed that for low curvature ratio the normalized mean velocity profile has a low dependency on Reynolds number as well as for increasing Reynolds number and high curvature ratio it tends to recover its fully developed shape [3]. Analysis of the developing turbulent flow through a three-dimensional 90° bend pipe with strong curvature has been studied by Min Chen and Zhiguo Zhang. Applying RNG k-epsilon model the flow structure was investigated as well as variation in pressure and velocity along the bend region was presented by the study. Their numerical result demonstrates that Dean motions co-exist with large scale swirling motions inside the bend pipe [4]. A certain Reynolds number of 4.45E04 is used by Abdelkrim Miloud et al. to investigate the turbulent flows through a u- bend pipe. Applying standard k-ϵ and the second moment closure RSM model they found that the secondary flows occur in the cross-stream half-plane of such configurations and primarily induced by high anisotropy of the cross-stream turbulent normal stresses near the outer bend [5]. Rana Roy Chowdhury et al. used standard k-ϵ model to examine the turbulent flow through 90-degree bend pipe with different curvature ratios. On this study the static pressure distributions along inner, outer wall and pressure loss factor for different curvature ratios and Reynolds number has been investigated and compared with experimental data. From the investigation they showed that the pressure distribution and pressure loss factor are dependent for different Reynolds number and curvature ratio throughout the bend [6]. Detached Eddy Simulation (DES) turbulence model was employed by Yan Wang et al. to investigate the fluid flow through a 90-degree bend pipe with large curvature ratio. The simulation was carried out using Reynolds number range from 5000 to 20000. The pressure and velocity distribution, pressure drop, fluid flow

Published on November 29, 2017.
Md. S. Hossain was with Chittagong University of Engineering & Technology (Email:safayet_shawon@ymail.com)
Md. I. Hossain was with Chittagong University of Engineering & Technology (Email: ishti_hossain@yahoo.com)
S. Pramanik was with Chittagong University of Engineering & Technology (Email: sonikg14@gmail.com)
Dr. J.U. Ahamed is with Chittagong University of Engineering & Technology (Email: jamal@cuet.ac.bd)

as well as secondary flow along the curved pipe were illustrated in this analysis. From their numerical investigation it is known that large curvature ratio makes the internal flow more complicated [7]. Muhammad Ahsan used a finite volume method (FVM) solver with k-ϵ turbulence model and enhanced wall treatment to investigate the flow of water at different velocities with higher Reynolds number in a 3D pipe. The effects of Reynolds number on turbulence intensity, shear stress and friction factor is illustrated in this study [8]. The flow separation characteristics in pipe bends is illustrated by Prasun Dutta et al. by using high Reynolds number. They applied k-ε turbulence model to examine single phase turbulent flow through pipe bends. The influence of Reynolds number on flow separation and reattachment has been presented on this paper [9]. Tarek A. Mekhail et al. studied Gas-solid two-phase flow in a 90˚ square bend numerically using k-ε turbulence model. The solid phase consists of glass spheres having mean diameter of 77 μm and the spheres are simulated with an air flowing at bulk velocity of 10 m/s. They compare the velocity field with and without injected glass particles of different diameter to observe the influence of glass particles on fluid flow [10]. Prasun Dutta and Nityananda Nandi carried out an investigation using k-ϵ model to show the influence of bend curvature on both axial velocity and static pressure distribution at different sections inside of pipe bend as well as adjacent sections of bend inlet (upstream) and outlet (downstream). On their study they tried to show that the velocity increases as the curvature ratio increases and found maximum velocity near the outlet section [11]. Using glass spheres as solid phase with mean dimeter of 77 m inside of a 90-degree square bend pipe where air was flowing at a bulk velocity of 10 m/s William Yang and Benny Kuan examined the Mean and turbulent flow properties for gas and particulate phases with the aid of 2D laser Doppler anemometry. In their study, due to considerable positive slip velocity between the two phases significant gas–solid separation was detected near the outer wall of the duct. They also found the velocity fluctuations in the solid phase was higher than that of the gas phase at the bend entrance [12]. Sowjanya Vijiapurapu and Jie Cui studied the fully-developed turbulent flows in circular pipes roughened by repeated square ribs with various spacing. In this study different RANS models such as standard k-ε, standard k-ω, Reynolds stress model and LES model were employed to solve the Reynolds-averaged Navier–Stokes equations and the models performed equally well in predicting the time-averaged flow statistics [13]. The effect of guide vane installed in the bend portion, in flow separation and velocity distribution for incompressible turbulent flow through 90-degree pipe bend was investigated by Sumit Kumar Saha and Nityananda Nandi. Using k-epsilon turbulence model and a particular Reynolds number several data had been collected for four different position of guide vane as well as flow separation and velocity distribution were found at different position on the bend pipe [14]. Leo H. O. Hellstrom et al. showed Dean motions downstream of the bend of a 90° bend pipe are very weak in the mean, and time resolved stereoscopic PIV demonstrates that the Dean motions co-exist with large scale swirling motions that switch sign and do not contribute to the mean [15]. Manish Kumar Rathore et al. compared different hydrodynamic performance characteristics of a straight pipe and a 90° bend pipe employing finite volume approach. Using a wide range of Reynolds number, the flow separation and the boundary layer separation has been analyzed. According to the friction factor at the bend section the inner and outer surface has unsymmetrical pattern and turbulent intensity also varies in comparison with straight pipe [16]. k-ε RNG turbulence model with standard wall function is used by Prasun Datta and N. Nandi to investigate the pressure drop characteristics of turbulent flow through 90-degree pipe bends. In this paper, the writers tried to provide cost effective solutions to design of the pipe bends based on the investigation of the pressure distribution and pressure drop characteristics over a wide range of Reynolds number. They also study the pressure loss coefficient in terms of Reynolds number and curvature ratio for the designing purpose [17].

CFD has developed into an inherent part of the analysis and design environment to predict performance of new designs or processes before they are implemented. Computational Fluid Dynamics (CFD) provides qualitative prediction of fluid flows by means of mathematical modeling and computer based solver. CFD simulation dramatically decrease the overall expense alongside increasing the speed. CFD offers the capability to examine specific phenomena for study for hypersonic flow or subsonic flow or adiabatic process etc. All of these results in more productivity. In this experiment, a widely used CFD package Fluent is used to analyze four different two equation turbulence model.

Turbulence is the three-dimensional unsteady random motion in fluid occurs at higher Reynolds number ($Re > 4000$). Almost all practical fluid flow in everyday life is turbulent. The boundary layers around and the wakes after different vehicle's movement such as aeronautical vehicles, aircraft and automobiles are turbulent. The typical flow around bluff bodies such constructions is turbulent. Two-equation turbulence models describe the turbulent length and time scale by solving two separate transport equations. The k-ϵ model is perhaps the most common turbulence model that used to calculate practical flow because of its higher accuracy and robustness. The standard k-ϵ model [18] presents the transport equations for the turbulence kinetic energy (k) and its dissipation rate (ϵ). The standard k-ϵ model is applicable only for fully turbulent flows. To improve its performance, couple of other variants of standard k-ϵ model have been introduced namely the RNG k-ϵ model [19] and the realizable k-ϵ model [20]. The RNG-based k-ϵ turbulence model is derived from the instantaneous Navier-Stokes equations, using a mathematical technique called "renormalization group" (RNG) methods [21]. The realizable k-ϵ model proposed by Shih et al. [20] contains an alternative formulation for the eddy viscosity [22]. It presents a modified transport equation for dissipation (ϵ) based on the dynamic equation of the mean-square vorticity fluctuation. The standard k-ω model is an empirical model based on model transport equations for the turbulence kinetic energy (k) and the specific dissipation rate (ω), which can also be thought of as the ratio of ε to k [23]. The quality of the simulation can depend crucially on the selected turbulence model and it is

important to make the proper model choice as well as to provide a suitable numerical grid for the selected model.

II. Mathematical Modelling

In this study the fluid is presumed as incompressible and (1) and (2) are the mass conservation and the momentum equations respectively whereas f_i represents the external forces and v represents the kinematic viscosity [14].

$$\frac{\partial u_i}{\partial x_i} = 0 \tag{1}$$

$$\frac{\partial u_i}{\partial x_i} + \frac{\partial u_i}{\partial x_i} = f_i \frac{1}{\rho}\frac{\partial u_i}{\partial x_i} + v\frac{\partial^2 u_i}{\partial x_i \partial x_j} \tag{2}$$

A. Standard k-ϵ Model

In Standard k-ϵ model [18], the turbulence kinetic energy (k) is represented by the following transport equation:

$$\frac{\partial}{\partial t}(\rho k) + \frac{\partial}{\partial x_i}(\rho k u_i) = \frac{\partial}{\partial x_j}\left[\left(\mu + \frac{\mu_t}{\sigma_k}\right) + \frac{\partial k}{\partial x_j}\right] + G_k + G_b - \rho\epsilon - Y_m + S_k \tag{3}$$

And, the dissipation rate ϵ is obtained from the following equation:

$$\frac{\partial}{\partial t}(\rho \varepsilon) + \frac{\partial}{\partial x_i}(\rho \varepsilon u_i) = \frac{\partial}{\partial x_j}\left[\left(\mu + \frac{\mu_t}{\sigma_\varepsilon}\right) + \frac{\partial \varepsilon}{\partial x_i}\right] + C1\varepsilon\frac{\varepsilon}{k}(G_k + C_{3\varepsilon}G_b) - C_{2\varepsilon}\rho\frac{\varepsilon^2}{k} + S_\varepsilon \tag{4}$$

G_k represents the generation of turbulence kinetic energy due to the mean velocity gradients and computed as mentioned in (5),

$$G_k = -\rho\overline{u_i' u_j'}\frac{\partial u_j}{\partial x_i} \tag{5}$$

G_b is the generation of turbulence kinetic energy due to buoyancy which is calculated by the following equation:

$$G_b = \beta g_i \frac{\mu_t}{Pr_t}\frac{\partial T}{\partial x_i} \tag{6}$$

B. RNG k-ϵ Model

The RNG $k-\epsilon$ model is slightly similar to the Standard k-ϵ model [21]. The governing equations of RNG $k-\epsilon$ model are stated as following:

$$\frac{\partial}{\partial t}(\rho k) + \frac{\partial}{\partial x_i}(\rho k u_i) = \frac{\partial}{\partial x_j}\left(\alpha_k \mu_{eff}\frac{\partial k}{\partial x_j}\right) + G_k + G_b - \rho\varepsilon - Y_M + S_k \tag{7}$$

$$\frac{\partial}{\partial t}(\rho \varepsilon) + \frac{\partial}{\partial x_i}(\rho \varepsilon u_i) = \frac{\partial}{\partial x_j}\left(\alpha_\varepsilon \mu_{eff}\frac{\partial \varepsilon}{\partial x_j}\right) + C_{1\varepsilon}\frac{\varepsilon}{k}(G_k + C_{3\varepsilon}G_b) - C_{2\varepsilon}\rho\frac{\varepsilon^2}{k} - R_\varepsilon + S_\varepsilon \tag{8}$$

C. Realizable k-ϵ Model

The transport equations for Realizable k-ϵ Model are as following [22]:

$$\frac{\partial}{\partial t}(\rho k) + \frac{\partial}{\partial x_i}(\rho k u_i) = \frac{\partial}{\partial x_j}\left[\left(\mu + \frac{\mu_t}{\sigma_k}\right) + \frac{\partial k}{\partial x_j}\right] + G_k + G_b - \rho\epsilon - Y_m + S_k \tag{9}$$

$$\frac{\partial}{\partial t}(\rho \varepsilon) + \frac{\partial}{\partial x_i}(\rho \varepsilon u_j) = \frac{\partial}{\partial x_j}\left[\left(\mu + \frac{\mu_t}{\sigma_\varepsilon}\right) + \frac{\partial \varepsilon}{\partial x_i}\right] + \rho C_1 S_\varepsilon - \rho C_2 \frac{\varepsilon^2}{k+\sqrt{v\varepsilon}} + C_{1\varepsilon}\frac{\varepsilon}{k}C_{3\varepsilon}G_b + S_\varepsilon \tag{10}$$

Where C_1, η and S are constants and these constants can be calculated by using (11), (12) and (13).

$$C_1 = \max\left[0.43, \frac{\eta}{\eta+5}\right] \tag{11}$$

$$\eta = S\frac{k}{\varepsilon} \tag{12}$$

$$S = 2\sqrt{S_{ij}S_{ij}} \tag{13}$$

D. Standard k-ω Model

The standard $k-\omega$ model [23] is an empirical model based on model transport equations for the turbulence kinetic energy (k) and the specific dissipation rate (ω). The transport equations of this model are as following:

$$\frac{\partial}{\partial t}(\rho k) + \frac{\partial}{\partial x_i}(\rho k u_i) = \frac{\partial}{\partial x_j}\left(\Gamma_k \frac{\partial k}{\partial x_j}\right) + G_k - Y_k + S_k \tag{14}$$

$$\frac{\partial}{\partial t}(\rho \omega) + \frac{\partial}{\partial x_i}(\rho \omega u_i) = \frac{\partial}{\partial x_j}\left(\Gamma_\omega \frac{\partial \omega}{\partial \omega_j}\right) + G_\omega - Y_\omega + S_\omega \tag{15}$$

In these equations, G_k represents the generation of turbulence kinetic energy. Γ_k and Γ_ω represent the effective diffusivity of k and ω respectively and can be measured by using (16) and (17). The effective diffusivities for the $k-\omega$ model are given by

$$\Gamma_k = \mu + \frac{\mu_t}{\sigma_k} \tag{16}$$

$$\Gamma_\omega = \mu + \frac{\mu_t}{\sigma_\omega} \tag{17}$$

E. Solver Setup

In this study the PISO algorithm was employed for pressure-velocity coupling. Although this algorithm requires slightly more processing time, it can dramatically decrease the total number of iterations required for convergence. For first run, first order upwind scheme was chosen for discretization setup. But for further accuracy, in terms of turbulent kinetic energy and turbulent dissipation rate, second order upwind scheme was given preference. Neighbor and skewness correction factor was set as 1.

III. Grid Generation

The relative size of the proposed model is shown Fig. 1(a). The geometry was divided into three sub-domains. The surface area of inlet and outlet section are equal to each other. The curvature ratio is 0.25. The grid was generated by quadrilateral elements whereas number of nodes and elements were 68476 and 67500 respectively. Enlarged grid at the bend region is shown in Fig. 1(b). Advanced size

function was utilized on curvature. Curvature normal angle and growth rate were 18 degrees and 1.20 respectively. Aspect ratio was obtained up to 1.1003. Mapped faced meshing was utilized to further improve the mesh quality.

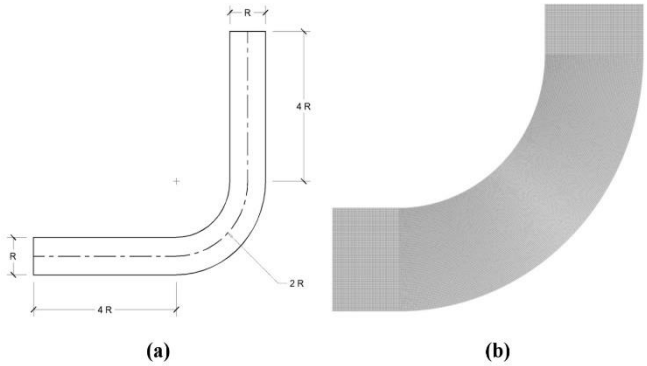

Fig. 1. Schematic diagram and enlarged grid at the bend region

IV. Result and Discussion

In this study numerical simulation were performed to investigate the deviation in turbulent kinetic energy, turbulent dissipation rate, eddy viscosity and turbulent intensity with the increase in Reynolds number for each numerical model. Ten sample of Reynolds number were taken to calculate each mathematical model. The inlet velocity was changed from 1.5 m/s to 6 m/s with the increase in 0.5 m/s. each of these analyses was performed under same boundary condition and using same solver (PISO) and discretization method (second order upwind). TKE, dissipation rate and eddy viscosity increased with Reynolds number and intensity decreased with the increase in Reynolds number. It was seen from Fig. 2 that, all the previously mentioned turbulent properties obtained from Standard k-ϵ model, deviates way much higher than the Realizable k-ϵ model, RNG k-ϵ model and Standard k-ω model. The turbulent properties obtained from Standard k-ω model were not shown in graphs as they were almost coincided with others.

The deviation found in Standard $k-\omega$ model is shown in Table Ⅰ. TKE (k) obtained from $k-\omega$ model increased slightly from the TKE obtained from Realizable $k-\epsilon$ model. Also the turbulent dissipation rate (ϵ) obtained from $k-\omega$ model increased slightly from the ϵ obtained from RNG $k-\epsilon$ model. The turbulent intensity decreased from Realizable $k-\epsilon$ model. The eddy viscosity decreased from the RNG $k-\epsilon$ model. At various sample of inlet velocity, TKE obtained from Realizable $k-\epsilon$ and Standard $k-\omega$ almost identical to each other. In this investigation, it is seen that, with the increase in Reynolds number, the difference between TKE obtained from Standard $k-\omega$ and Realizable $k-\varepsilon$ model is lessening gradually. At $R_e = 74E03$, TKE obtained from Standard $k-\omega$ model increased by 6.44% from Realizable $k-\epsilon$ model whereas at $R_e = 298E03$, TKE obtained from Standard $k-\omega$ model increased by 1.88% from Realizable $k-\epsilon$ model. Also, with the increasing Reynolds number, turbulent dissipation rate obtained from RNG $k-\epsilon$ and Standard $k-\omega$ almost coincided. The difference between turbulent dissipation rate obtained from Standard $k-\omega$ and RNG $k-\varepsilon$ model is slowly decreasing with the increase in inlet velocity. At $R_e = 74E03$, turbulent dissipation rate obtained from Standard $k-\omega$ model increased by 6.16% from RNG $k-\epsilon$ model whereas at $R_e = 298E03$, TKE obtained from Standard $k-\omega$ model increased by 3.04% from RNG $k-\epsilon$ model.

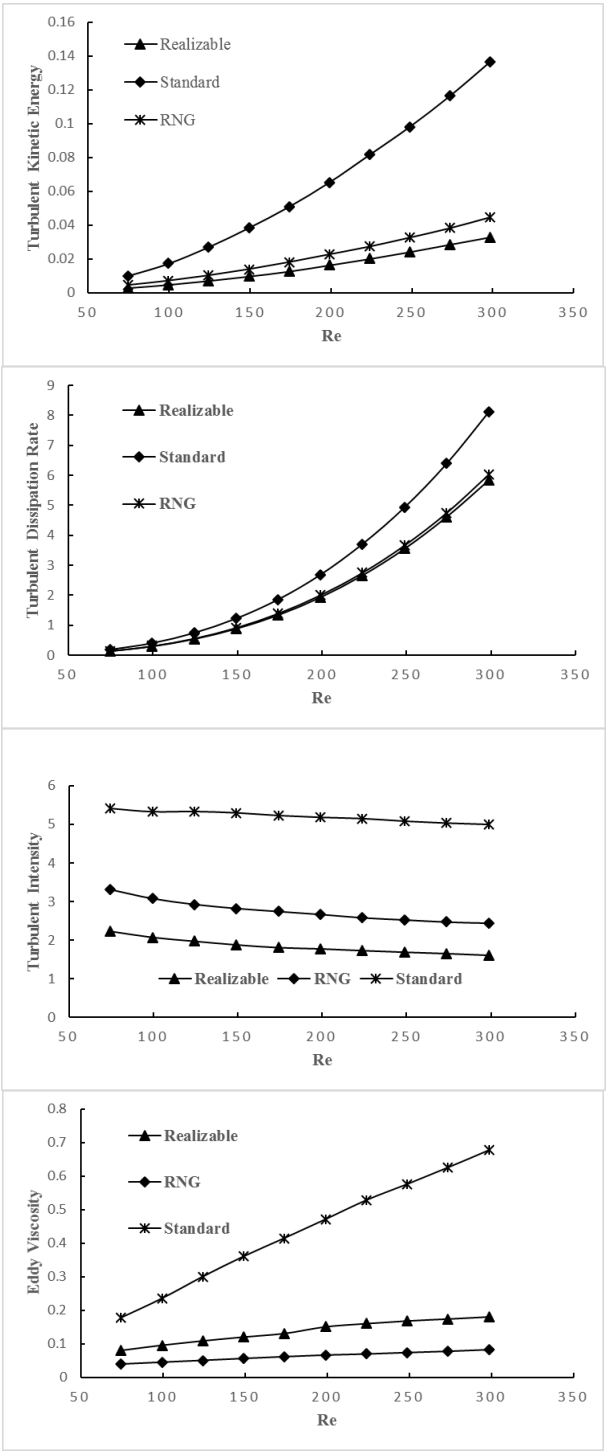

Fig. 2. Change in turbulence property under different k-ϵ turbulence models

Although, each of the previously mentioned turbulent properties are much higher in Standard $k-\epsilon$ model, the skin friction factor obtained at bend region, deviates in very little amount from other turbulence model. Graphically they almost coincide with each other. Table II depicts the differences in skin friction factor among different models for each sample of Reynolds number.

TABLE I: VARIATION FOUND IN K − ϵ MODEL

Reynolds Number (R_e)	Turbulent Kinetic Energy (%)	Turbulent Dissipation Rate (%)	Turbulent Intensity (%)	Eddy Viscosity (%)
74.64107677	6.442107392	6.157595693	18.2595875	46.28528113
99.52143569	6.006563417	5.841770924	17.59780506	43.41190886
124.4017946	3.263948101	5.148442533	18.81406909	43.64747416
149.2821535	3.811670965	4.723859611	17.80783135	42.3278282
174.1625125	3.423276373	4.151419368	17.63281095	42.3658145
199.0428714	1.489595359	3.872621656	18.11995188	40.82859288
223.9232303	1.207551379	3.790738988	17.86125929	38.71689451
248.8035892	0.930277919	3.52665178	17.64969179	37.89210058
273.6839482	1.024540191	3.41426829	17.18284477	36.37786262
298.5643071	1.876849121	3.040081582	16.41019447	36.52725352

TABLE II: VARIATION IN SKIN FRICTION FACTOR UNDER DIFFERENT MATHEMATICAL MODEL

Reynolds Number (R_e)	Standard k − ω (%)	Realizable k − ϵ (%)	RNG k − ϵ (%)
74.64107677	3.099003023	4.801429026	4.659292445
99.52143569	2.346578766	3.820701674	4.109217319
124.4017946	1.829963095	3.10363723	3.69218458
149.2821535	1.61145332	2.6370514	3.450910704
174.1625125	1.519008206	2.35644899	3.320029772
199.0428714	1.487291399	2.173751735	3.198788226
223.9232303	1.44427813	2.003798502	3.072100498
248.8035892	1.457748973	1.912593543	3.033909477
273.6839482	1.472721581	1.827244557	2.985616131
298.5643071	1.464742706	1.724922398	2.956171523

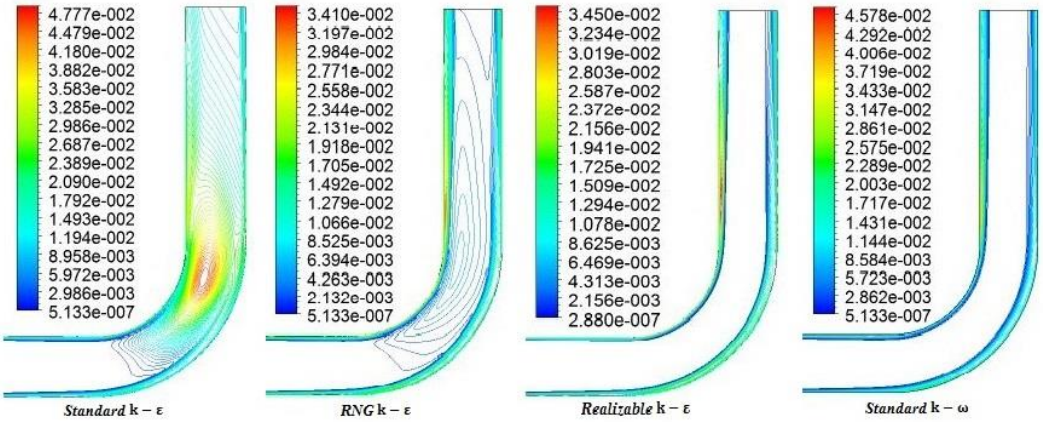

Fig. 3. Contour of turbulent kinetic energy for $R_e = 74E03$

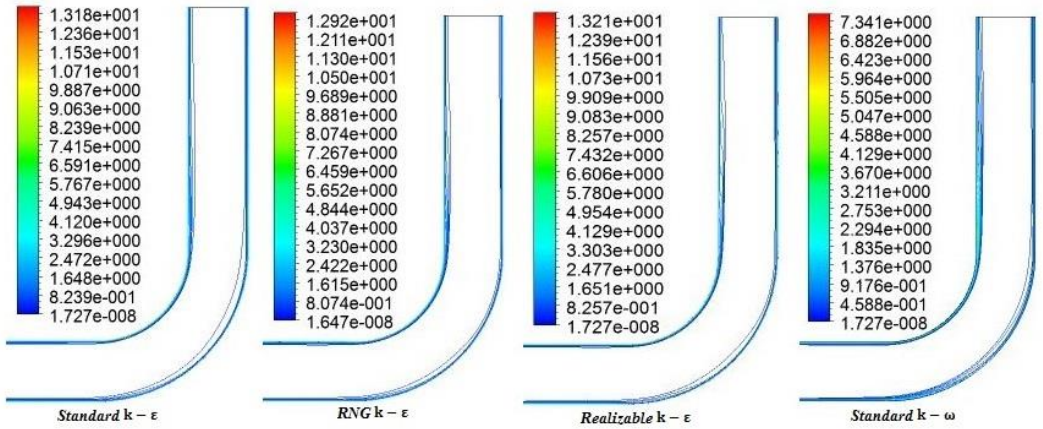

Fig. 4. Contour of turbulent dissipation rate for $R_e = 74E03$

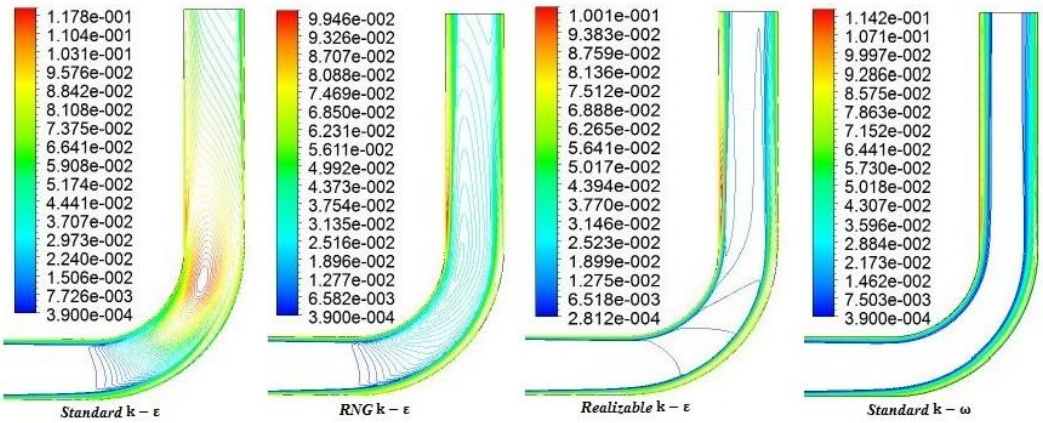

Fig. 5. Contour of turbulent intensity for $R_e = 74E03$

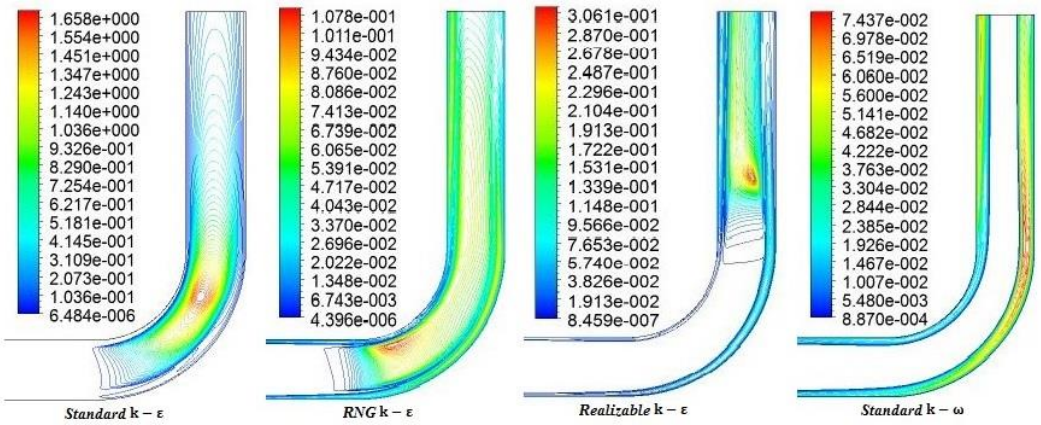

Fig. 6. Contour of eddy viscosity for $R_e = 74E03$

Fig. 3 depicts the variation of TKE in contour band for each numerical model for $R_e = 74E03$. The contour profile differs very little from each other in Realizable $k-\epsilon$ model and Standard $k-\omega$ model. It has been found that under the same boundraty condition Standard $k-\epsilon$ prsennted most diverse contour profile. Fig. 4 represents the variation of turbulent dissipation rate in contour band for each numerical model for $R_e = 74E03$.Turbulent dissipation rate mainly affected the boundary area under each model for lower to higher sample of Reynolds number. Fig. 5 represents the variation of turbulent intensity in contour band for each numerical model for $R_e = 74E03$. Under the same boundary condition, the increase in Reynold number, affects each of these mathematical model differently as per expectation. Although the change is more steady in case of Standard $k-\omega$ model with higher Reynolds number. Fig. 6 shows the variation of eddy viscosity in contour band for each numerical model for $R_e = 74E03$. It has been observed that for each sample of Reynolds number, the eddy viscosity obtained from all the $k-\varepsilon$ turbulent models, affects the flow from bend region to the outlet section whereas, in the Standard $k-\omega$ turbulent model, the eddy viscosity mainly affects the flow near the boundary region.

REFERENCES

[1] Jongtae Kim, Mohan Yadav and Seungjin Kim, "Characteristics of secondary flow induced by 90-degree elbow in turbulent pipe flow," Engineering Applications of Computational Fluid Mechanics Vol. 8, No. 2, pp. 229–239 (2014).

[2] Beibei Feng, Shiming Wang, Shengqiang Li, Xingtuan Yang, and Shengyao Jiang, "Experimental and numerical study on pressure distribution of 90° elbow for flow measurement," Hindawi Publishing Corporation, Science and Technology of Nuclear Installations, Volume 2014, Article ID-964585.

[3] Prasun Dutta and Nityananda Nand, "Effect of Reynolds Number and curvature ratio on single phase turbulent flow in pipe bends," Mechanics and Mechanical Engineering, Vol. 19, No. 1 (2015)

[4] Min Chen and Zhiguo Zhang, "Numerical simulation of turbulent driven secondary flow in a 90° bend pipe," Advanced Materials Research Vols. 765-767 (2013) pp 514-519.

[5] Abdelkrim Miloud, Mohammed Aounallah, Mustapha Belkadi, Lahouari Adjlout, Omar Imine and Bachir Imine, "Turbulent flow computation in a circular U-Bend," EPJ Web of Conferences 67, 02075 (2014).

[6] Rana Roy Chowdhury, Suranjan Biswas, Md. Mahbubul Alam and A. K. M. Sadrul Islam, "Turbulent flow analysis on bend and downstream of the bend for different curvature ratio," AIP Conference Proceedings 1754, 040020 (2016).

[7] Yan Wang, Quanlin Dong, and Pengfei Wang, "Numerical investigation on fluid flow in a 90-degree curved pipe with large curvature ratio," Hindawi Publishing Corporation Mathematical Problems in Engineering Volume 2015, Article ID 548262.

[8] Muhammad Ahsan, "Numerical analysis of friction factor for a fully developed turbulent flow using $k-\varepsilon$ turbulence model with enhanced wall treatment," Beni - Suef University journal of basic and applied sciences 3(2014) 269 e277.

[9] Prasun Dutta, Sumit Kumar Saha, Nityananda Nandi and Nairit Pal, "Numerical study on flow separation in 90° pipe bend under high Reynolds number by k-ε modelling," Engineering Science and Technology, an International Journal 19 (2016) 904–910.

[10] Tarek A. Mekhail, Walid A. Aissa, Soubhi A. Hassanein, and Osama Hamdy, "CFD simulation of dilute gas-solid flow in 90˚ square bend," Energy and Power Engineering, 2011, 3, 246-252.

[11] Prasun Dutta and Nityananda Nandi, "Effect of bend curvature on velocity & pressure distribution from straight to a 90° pipe bend - A Numerical Study," REST Journal on Emerging trends in Modelling and Manufacturing 2(4) 2016, 103-108.

[12] William Yang and Benny Kuan, "Experimental investigation of dilute turbulent particulate flow inside a curved 90◦ bend," Chemical Engineering Science 61 (2006) 3593–360.

[13] Sowjanya Vijiapurapu and Jie Cui, "Performance of turbulence models for flows through rough pipes," Applied Mathematical Modelling 34 (2010) 1458–1466.

[14] Sumit kumar saha and Nityananda nandi, "Change in flow separation and velocity distribution due to effect of guide vane installed in a 90° pipe bend," Mechanics and Mechanical Engineering Vol. 21, No. 2 (2017) 353–361 Lodz University of Technology.

[15] Leo H. O. Hellstrom, Metodi B. Zlatinov, Alexander J. Smits and Guongjun Cao, "Turbulent pipe flow through a 90° bend." Seventh International Symposium on Turbulence and Shear Flow Phenomena 2011.

[16] Manish Kumar Rathore, Dilbag Singh Mondloe and Satish Upadhyay, "Computational Investigation of Fluid Flow 90° Bend Pipe Using Finite Volume Approach," International Research Journal of Engineering and Technology (IRJET), Volume: 04 Issue: 06, June - 2017.

[17] P. Dutta and N. Nandi, "Study on pressure drop characteristics of single phase turbulent flow in pipe bend for high Reynolds number," ARPN Journal of Engineering and Applied Sciences, Vol. 10, no. 5, March 2015.

[18] B. E. Launder and D. B. Spalding. "Lectures in Mathematical Models of Turbulence." Academic Press, London, England. 1972.

[19] V. Yakhot and S. A. Orszag. "Renormalization Group Analysis of Turbulence I Basic Theory". Journal of Scientific Computing. 1(1). 1–51. 1986.

[20] T.-H. Shih, W. W. Liou, A. Shabbir, Z. Yang, and J. Zhu. "A New $k-\varepsilon$ Eddy-Viscosity Model for High Reynolds Number Turbulent Flows - Model Development and Validation". Computers Fluids. 24(3). 227–238. 1995.

[21] S. A. Orszag, V. Yakhot, W. S. Flannery, F. Boysan, D. Choudhury, J. Maruzewski, and B. Patel. "Renormalization Group Modeling and Turbulence Simulations". In International Conference On Near-Wall Turbulent Flows, Tempe, Arizona. 1993.

[22] W. C. Reynolds. "Fundamentals of turbulence for turbulence modeling and simulation". Lecture Notes for Von Karman Institute Agard Report No. 755. 1987.

[23] M. S. Solum, R. J. Pugmire, and D. M. Grant. "Energy and Fuels." 3. 187. 1989.

Md. Safayet Hossain was born in Bangladesh. He obtained BSc in Mechanical Engineering from Chittagong University of Engineering & Technology in 2017. His field of interest includes aerodynamics. computational fluid dynamics and renewable energy. He has published a number of publications on different academic journals.

Md. Ishtiaque Hossain was born in Bangladesh. He accomplished BSc in Mechanical Engineering from Chittagong University of Engineering & Technology in 2017. His research interest is in computational fluid dynamics, heat transfer, renewable energy, sustainable energy and thermodynamics.

Somit Pramanik was born in Bangladesh. He obtained BSc in Mechanical Engineering from Chittagong University of Engineering & Technology in 2017. His research interest is in aerodynamics, fluid dynamics, renewable energy and sustainable energy.

Dr. Jamal Uddin Ahamed was born in Bangladesh. He obtained his PhD from University of Malaya in 2012. He is a professor in Chittagong University of Engineering & Technology. His research interest primarily includes effect of Nano fluid in refrigeration heat transfer performance, exergy analysis of vapor compression system and Nano technology in refrigeration and air conditioning system. He published numerous publications on different academic journals.